International Journal of Multiphysics
Volume 18, No. 4, 2024
ISSN: 1750-9548

Assessment of the Influence of Alkali-Silica Reaction (ASR) and Elevated Temperatures on the Fracture Mechanics of Reinforced Concrete Beams with Varying Stirrup Spacings.

Salim Hashim Hussein[1], Amir Houshang Akhaveissy[2,] *, Bahaa Hussain Al-Abbas[3]

[1] Candidate of Ph.D. student, Department of Civil Engineering, Faculty Engineering, Razi University, Kermanshah, Iran.

[2] Associate Professor, Department of Civil Engineering, Faculty Engineering, Razi University, Kermanshah, Iran.

[3] Assistant Professor, Department of Civil Engineering, Faculty Engineering, Kerbala University, Kerbala, Iraq.

*** Corresponding author:**

A.H. Akhaveissy, E-mail: Ahakhaveissy@razi.ac.ir

Abstract

The aim of our study was to investigate the effects of thermal influences, such as heating or fires, and alkali silica reaction on the resistance of girders. We examined these influences both individually and in combination. In addition, we also studied the impact of stirrups on the resistance of the girders. Three cases were considered for the beams: typical stirrup use, higher than typical stirrup use, and lower than typical stirrup use. The role of stirrups in each case was analyzed. Our results showed a decrease of 12%, 15%, and 18% in the test results when the specimens were exposed to elevated temperatures, ASR, and a combination of both, respectively. Furthermore, we found that the amount of secondary reinforcement has a significant effect on reducing the impact of these factors. This study contributes to our understanding of the behavior of concrete under the influence of ASR and elevated temperatures, providing valuable insights for improving the design and maintenance of structures exposed to these conditions. We also developed numerical models and compared them to the experimental results, which showed similar outcomes

Keywords:-ASR, heating, reinforced concrete beam, Stirrup Spacings, Fracture Mechanics

1. Introduction

The interaction between silica and alkali compounds significantly affects the behaviour and durability of reinforced concrete structures. Silica, present in the aggregate, and alkali compounds in the cement can chemically react in a process known as alkali-silica reaction (ASR) [1-2]. This reaction can lead to the formation of a gel-like substance that causes expansion and cracking in concrete over time. Additionally, exposure to high temperatures can result in thermal stresses that may affect the mechanical properties of concrete [3,4].

Through a series of chemical reactions, the alkalis found in the pore solution interact with silica present in amorphous or slightly crystallized phases within aggregates. These phases are initially attacked by hydroxyl ions. As a result of this reaction, new phases are formed within the porous structure of the concrete, causing it to swell. From a mechanical perspective, the effects of alkali-silica reaction (ASR) on concrete can be likened to an internal pressure. When the stress resulting from this pressure exceeds the local tensile strength, it leads to

irreversible cracking. Additionally, stresses on the concrete matrix from other sources also contribute to expansion, as they create preferred directions for the occurrence of cracks and subsequent damage [5].
model resides in its ability to treat interaction between rebars and concrete affected by the Alkali-Silica Reaction (ASR). The model is able to predict the anisotropic swelling induced by the combination of homogenized rebars and external loadings. An application to a well-documented laboratory test for reinforced concrete beams shows the ability of the model to assess residual strength capacity of the beam after a long period of ageing in a natural environment [6].
Numerous studies have been conducted to explore the individual effects of alkali-silica reaction and high temperatures on reinforced concrete structures [2-7]. Several studies have examined the impact of alkali-silica reaction on concrete elements, focusing on criteria such as compressive strength, tensile strength, and modulus of elasticity. The results have shown that alkali-silica reaction can significantly reduce the mechanical properties of concrete. The magnitude of this reduction varies depending on factors such as the degree of aggregate reaction, curing conditions, and duration of exposure to alkali-silica reaction [8,9].
Similarly, the effect of elevated temperatures on the behaviour of reinforced concrete has been extensively studied [10,11]. High temperatures can cause thermal expansion, resulting in microcracking, loss of strength, and changes in material stiffness. Studies have demonstrated that concrete exposed to high temperatures experiences a decrease in compressive strength, tensile strength, and modulus of elasticity. The extent of these effects depends on the temperature level and the duration of exposure [12-14].
Furthermore, researchers have investigated the combined effect of alkali-silica reaction and elevated temperatures on reinforced concrete elements. The interaction between these factors can lead to further deterioration in the mechanical properties of concrete. The presence of alkali-silica reaction in concrete can increase its susceptibility to damage when exposed to high temperatures, resulting in reduced strength and durability [1-8].
Additionally, the role of secondary reinforcement in reinforced concrete structures has been studied. Changing the amount of secondary reinforcement, whether increasing or decreasing it, can impact cracking behaviour, load-carrying capacity, and overall performance of reinforced concrete elements. The influence of these changes has been investigated in several studies worldwide, and the results have shown their effect on the properties of reinforced concrete [15].
With the increased likelihood of concrete being exposed to high temperatures, there is a growing focus on understanding its behaviour in relation to temperature effects. Experimental evidence suggests that temperature affects cracking behaviour in concrete. Many researchers have studied the effect of temperature on cracking parameters, particularly crack energy and material susceptibility to fracturing. Others have conducted tests on preheated notched beam specimens and found that crack energy increases initially with temperature and then decreases [7-12]. The effect of temperatures up to 450°C and testing conditions (hot and cold) on crack energy of high-performance concrete has been investigated. The results have shown that in hot concrete, crack energy exhibits a decrease followed by an increase with increasing temperatures, whereas in cold concrete, crack energy remains consistently high and then decreases. For example, Baymonti and Gambirova conducted tests on self-consolidating concrete (SCC) at temperatures ranging from 20°C to 600°C and found that the crack strength ratio decreased from 1 at 20°C to approximately 0.34 at 600°C. Similarly, Pan et al. found that geopolymer concrete exhibits a higher increase in crack strength at high temperatures compared to ordinary cement-based concrete, based on concrete strength tests [14].
Numerous previous studies have been conducted to explore the effects of the interaction between silica and alkali compounds as well as the effects of elevated temperatures on reinforced concrete. However, further research and investigations are needed to accurately understand the separate and combined effects of these factors on the mechanical properties of concrete and the impact of changes in secondary reinforcement.
This study aims to contribute regarding the separate and combined effects of alkali-silica reaction and elevated temperatures on the mechanical properties of reinforced concrete. The impact of each factor will be analysed individually and under combined influence, along with studying the effect of changes in secondary reinforcement through both increases and decreases on these properties. The results of this study are expected to provide valuable information for civil engineers, structural designers, and decision-makers in the fields of designing and constructing structures exposed to the effects of alkali-silica reaction and elevated temperatures.

International Journal of Multiphysics
Volume 18, No. 4, 2024
ISSN: 1750-9548

2. Material properties & specimens

2-1. Materials

In order to achieve the goal of the study, which is to analyze the effect of the interaction of alkalis, silica, and high temperatures, individually or in combination, on samples of reinforced concrete with varying amounts of secondary reinforcement.

All specimens used in this research were prepared with an identical mix design, which is explained in Table 1. This mix design employed Cement that satisfies the standard specified by Iraq, and its chemical composition is comprehensively presented in Table 2. The concrete mix design in this paper conducted in accordance with the American Concrete Institute (ACI) (211.1-91) [16]. The ordinary Portland cement (OPC) type (I) was used in the study supplied from Kerbala, Iraq, in accordance with (ASTM C150-18) [17]. The fine aggregate in the concrete mix consisted of natural sand obtained from Kerbala, Iraq, with a fineness modulus of (2.8), while the coarse aggregate crushed type from Kerbala, Iraq, with a size of (9.5) mm and a specific gravity of (2.58) were used, in accordance with (ASTM C33-03) [18]. To enhance workability with a minimal water content, a superplasticizer admixture commonly known as (sika viscocrete 905s) at a rate of (1%) by weight of the cement was used, in accordance with (ASTM C494-05) [19]. A Slump quantity of (75-100) mm was determined for normal concrete according to (ASTM C143) [20]. The gradation used in this study followed the specifications outlined in ASTM Cl260, as illustrated in the grading curve depicted in figure 1.

The test specimens were produced using a high-precision wooden mold that was completely coated with a special oil before pouring the concrete. After being poured into the molds, the concrete was allowed to set for 24 hours before the molds were opened. The specimens were then cured for 28 days under standard laboratory conditions. after which they were returned to the $(NaOH)$ solution at 80°C for an additional 14 days according to ASTM C1260. The next step involved placing both the standard and ASR samples inside the oven and gradually increasing the temperature until it reached 700 degrees Celsius Figure 2 shows the relationship between temperature and time that was applied to the samples for the experimental and numerical cases, where the temperature was raised first and then hibernated at a specific temperature for a period of time shown in the diagram.

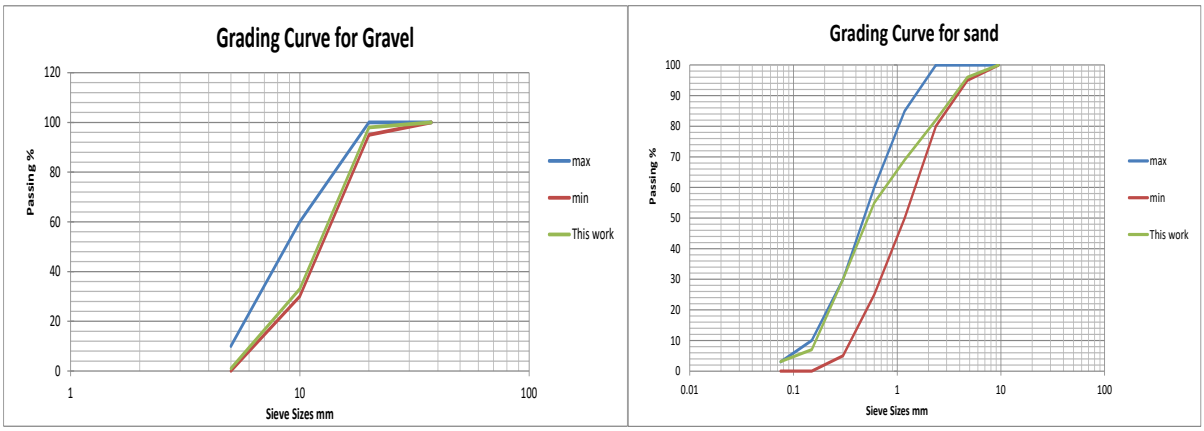

Fig1. Grading curve of sand and gravel used for concrete mixes

Table 1. Mix proportions of concrete and compressive strength (kg/m3)

MIX	Cement (Kg)	Coarse Aggregate (Kg)	Fine Aggregate (Kg)	w/c	Sika-viscocrete 905 S (%)	Compressive Strength (MPa)
M1	420	1080	800	0.42	1	56

Table 2. Chemical constituent of cement (%)

SiO2	Al2O3	Fe2O3	CaO	MgO	SO3	K2O	Losson Ignition
21.6	5.51	3.94	63.18	1.65	2.71	0.90	1.17

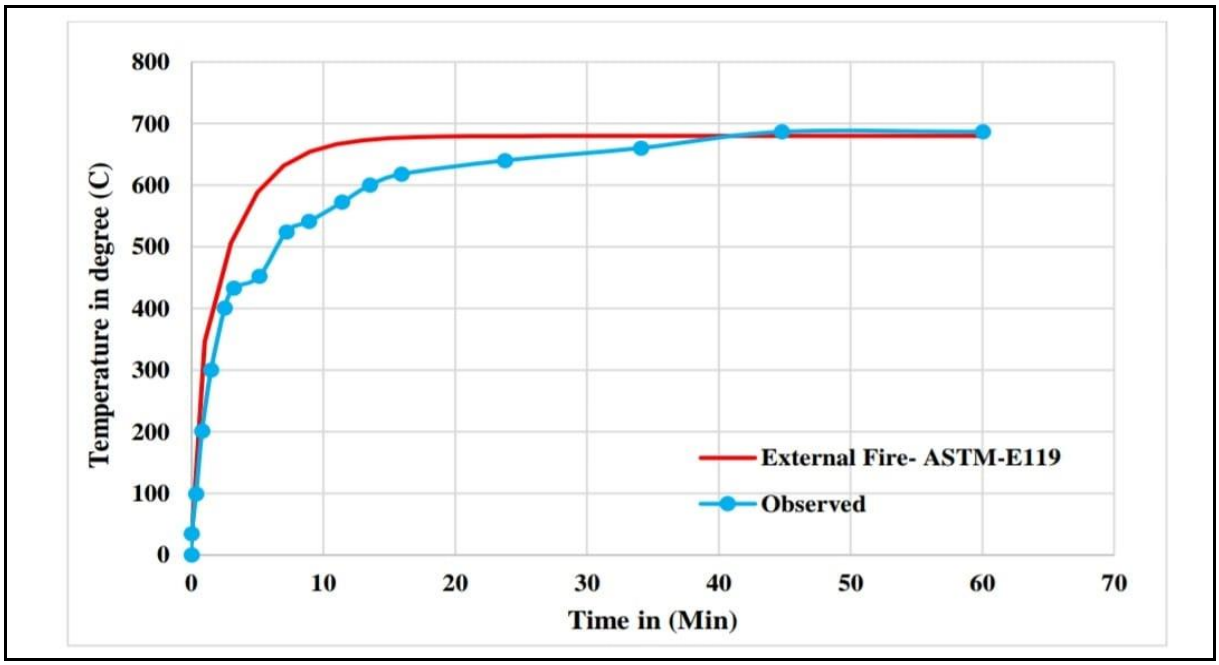

Fig2. the relationship between temperature degree and Time

2-2. Test procedure and instrumentation

Specimens with dimensions of 120x200x1400mm, where three different types of reinforced concrete beams (B1, B2, B3: where is B2 is the Standard ratio of secondary reinforcement, B3 less than it B1 is more than it figure 3, were cast with respect to the variation in the quantity of secondary reinforcement where it has been arranged into four groups The shape and dimensions of the specimens are presented in Figures 3 and 4, and their number and designation are listed in Table 4. Cubic specimens measuring 150x150x150mm were also employed to establish the compressive strength of the concrete. After 28 days of curing, the compressive strength of the concrete was found to be 56 MPa. The detailing of the reinforcement for all samples was designed according to ACI (352R-02) [21]. Table 3, represents the physical properties of reinforcement steel bars according to (ASTM A615/A615M-15) [22].

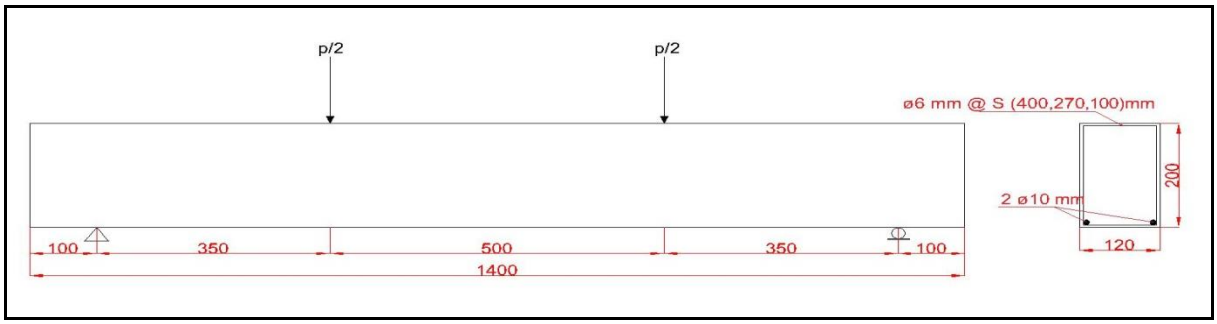

Fig3. Details of beams

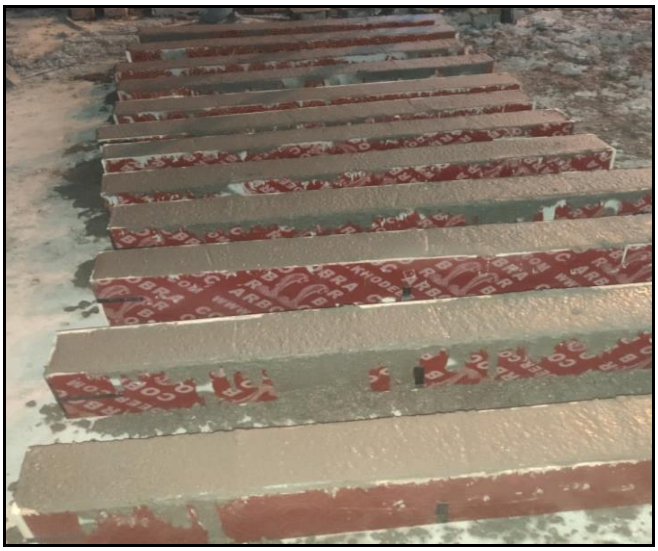

Fig4. Sketch of fracture testing specimen

Table 3 - Physical properties of steel bars

Diameter of bars (mm)	Cross sectional area, (mm^2)	Yield strength (MPa)	Tensile strength (MPa)	Maximum tensile strain (%)	Elastic modulus (GPa)
6	28.26	285	415	8	198
10	78.50	310	420	8	200

Table 4. The specimen number and dimensions

Series	Description	LxBxH(mm)	Number of specimens
G1 (B1, B2, B3)	Standard	1400x120x200	**3**
G2 (B1, B2, B3)	Heated	1400x120x200	**3**
G3 (B1, B2, B3)	Alkali-silica reaction	1400x120x200	**3**
G4 (B1, B2, B3)	Heated and Alkali-silica reaction	1400x120x200	**3**

To carry out the experiments, the samples to be tested were prepared by casting the concrete beams using the appropriate mixture and placing them in the designated molds. The required specifications regarding water ratios and curing time should be followed. high-rigidity steel frame is used to provide support for the concrete beams during the test. The testing process was carried out through a testing device that applies two concentrated forces at a distance from the centre of the supported beam in two different positions, as shown in the figure 5. The frame should be stable and sturdy to prevent any undesirable deformation during loading. A 200-kilonewton load cell is used to measure the applied load on the concrete beams. The load cell converts the applied force into an electrical signal, enabling precise load measurements.

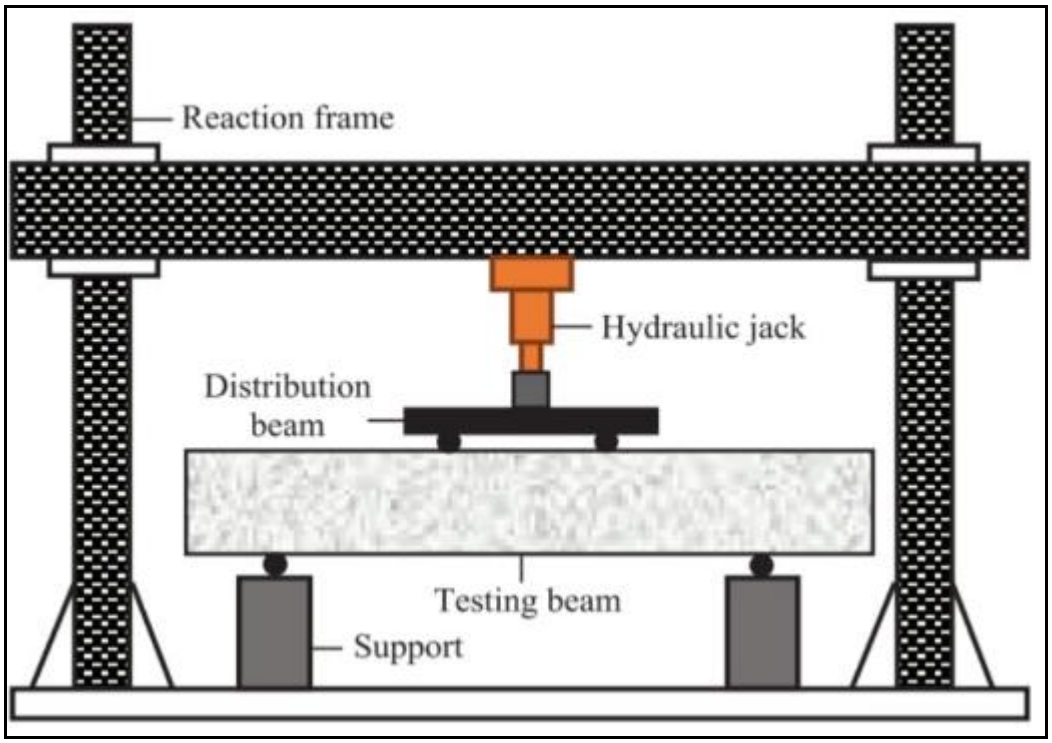

Fig5. Experimental test device

For displacement measurement an LVDT (Linear Variable Differential Transformer) is utilized to measure the deformation in the concrete beams during loading. The LVDT converts the longitudinal deformation into an electrical signal that can be accurately measured.

The load cell and LVDT are calibrated before the tests to ensure measurement accuracy. The load cell and LVDT are adjusted and calibrated using known force and deformation standards to ensure accurate results.

The concrete beams are placed on the sturdy steel frame in a straight and stable manner. The experimental load is applied at the specified loading points, and the load and associated deformation are measured using the load cell and LVDT, respectively all details are shown in figure 6.

Fig6. The examination details

3. Results and discussion

3-1. Data Analysis and Mathematical Equations

Flexural strength, also known as fracture energy or critical release rate of energy, is a measure of a material's resistance to fracture or failure under bending. In the context of concrete, it refers to the energy required to

initiate and propagate cracks when a concrete beam or specimen is subjected to bending loads. When a concrete beam is loaded in bending, tensile stresses develop on the bottom surface of the beam, leading to the formation and propagation of cracks. Flexural strength represents the amount of work required to open and extend these cracks. It measures the ability of concrete to absorb and dissipate energy before failure occurs. Flexural strength is typically determined by measuring the area under the load-deflection curve obtained during a flexural test. It is calculated by integrating the curve and represents the total energy absorbed by the concrete specimen during the test [23-26].

The flexural strength of concrete can be calculated using the following equations:

$$P_{max} = \frac{3F_c' I}{2b} \quad (1)$$

Where: P_{max}: The maximum load at failure, Fc: the compressive strength of concrete.
I: the moment of inertia of the concrete section. b: the width of the concrete section.

Deflection calculation (Δ): The deflection is calculated using the following equation:

$$\Delta = \frac{5(P_{max} l^4)}{384EI} \quad (2)$$

where: L: the actual length of the concrete member. E: the modulus of elasticity of concrete.
I: the moment of inertia of the concrete section.

Flexural energy calculation (Gf): calculated using the following equation:

$$Gf = \left(\frac{1}{2}\right) \sigma_{max} \Delta \quad (3)$$

where: σ_{max}: the maximum stress in the concrete. Δ: the deflection.

High values of flexural strength indicate durability and higher resistance to fracture in concrete. It is an important parameter in evaluating the performance and durability of concrete structures, as it reflects the materials' ability to withstand applied loads and resist crack propagation. Understanding flexural strength in concrete is essential in design and engineering analysis, as it helps assess the behaviour of structures and predict potential failure modes for concrete elements subjected to bending or flexural loads [27-30].

3-2. Numerical simulations

Numerical simulations were conducted for the tested models using the ABAQUS software, and the experimental results were matched with the numerical models. It was found that the difference between them is not significant, and therefore, these models can be considered validated. The details of the simulation were avoided for brevity. Figures 7 to 9 present the simulation results.

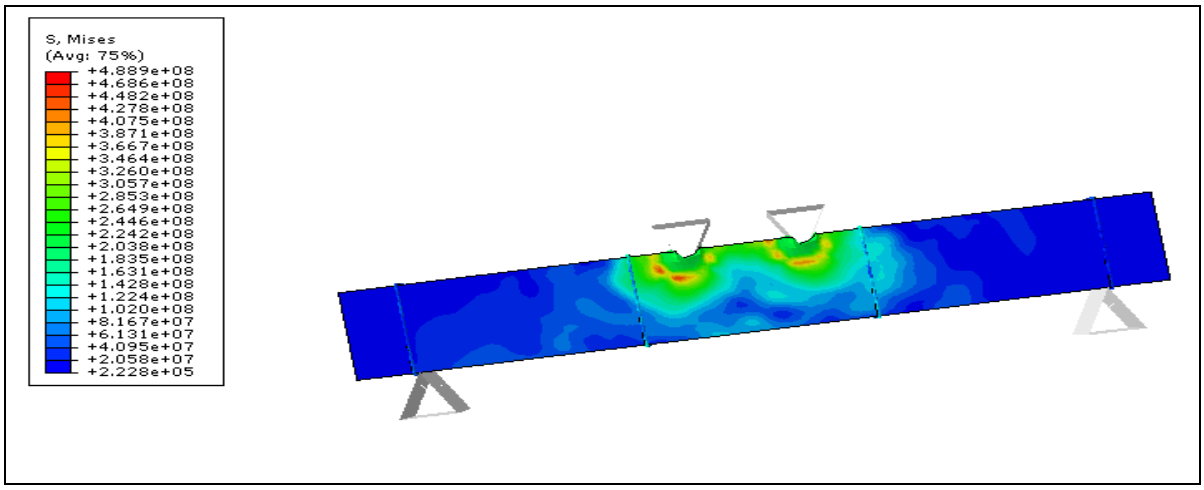

Fig7. presents an overview of the stress level under the application of bidirectional load

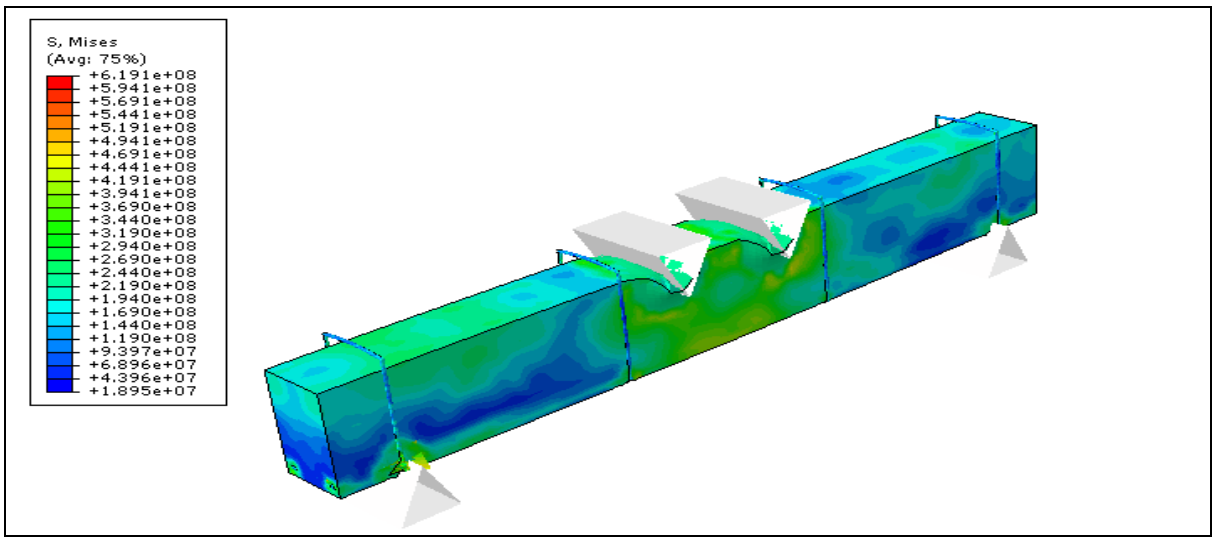

Fig8. depicts the fracture mechanics under the application of bidirectional load

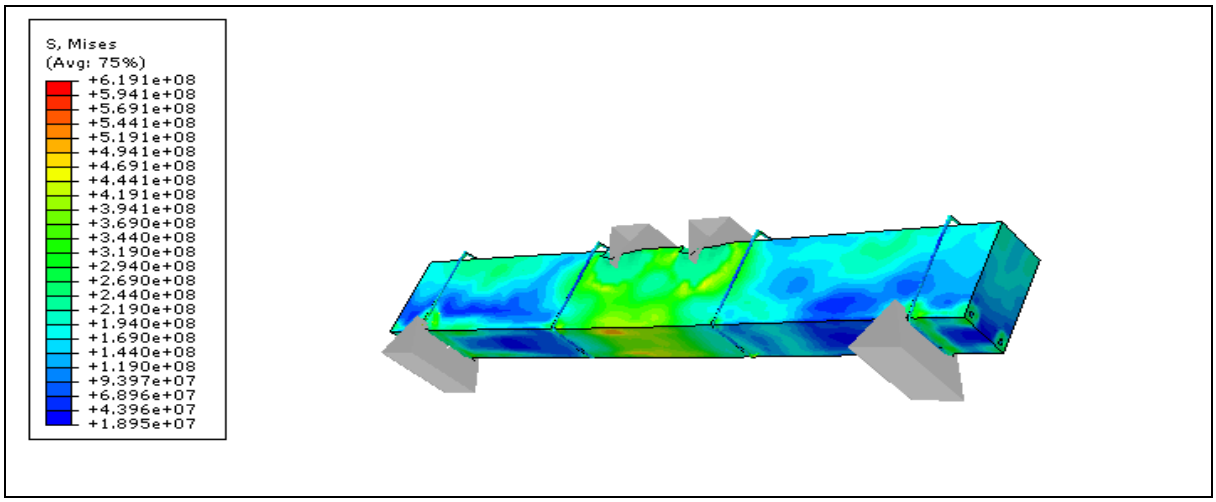

Fig9. provides insight into how openings impact tensile fracture in the context of applying bidirectional load

3-3. Experimental Results and Analysis

The experimental nature of the results obtained from the flexural strength and displacement diagram in reinforced concrete represents a crucial key to understanding material behavior and its engineering applications. This report aims to provide an overview of the main findings extracted from the flexural strength and displacement diagram, obtained from a series of laboratory experiments. The collected data will be reviewed and comprehensively analyzed to understand the details of the reinforced concrete interaction with various loads, such as bending, shear, and compression. This analysis aims to enhance our understanding of material behavior and improve the engineering design and analysis of structures subjected to such loads.

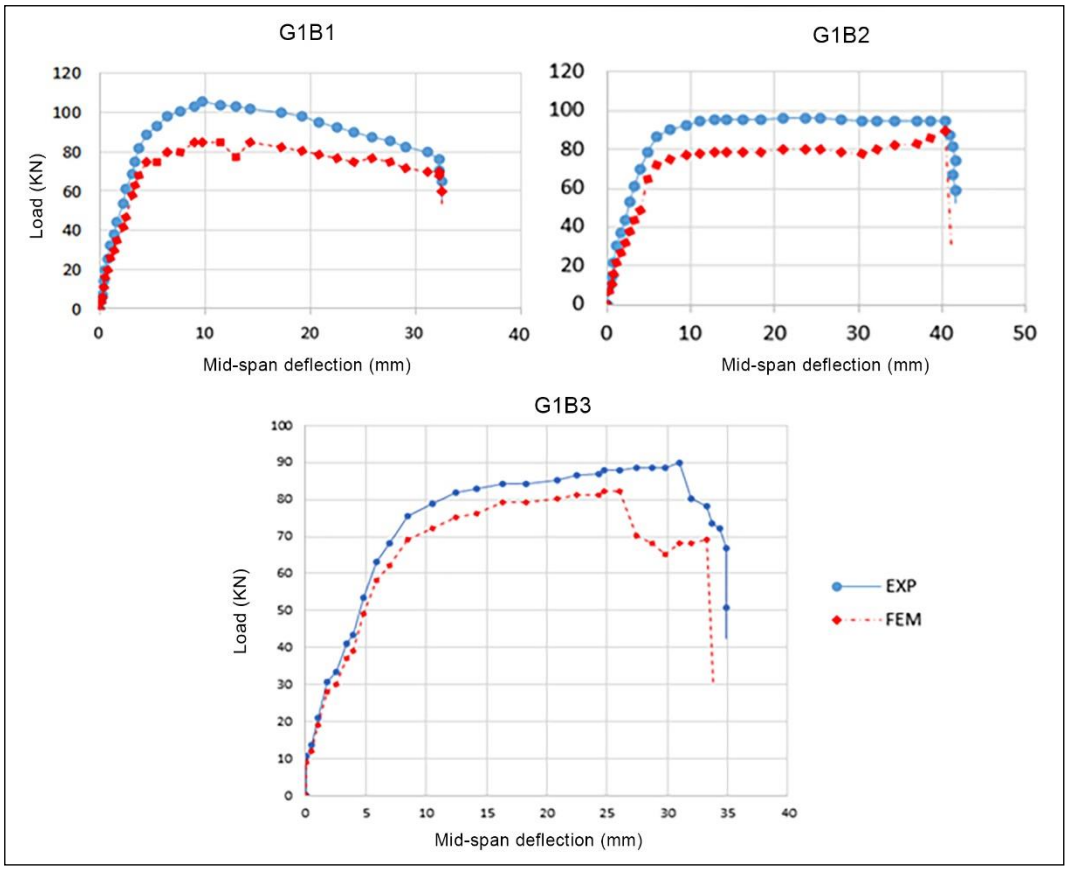

Fig10. illustrates the force-displacement (midpoint) graph for the first group G1

Figure 10 shows the case of studying beams without a thermal effect or (alkali-silica reaction) on the beam. This is the (G1) case, in order for there to be three cases of typical stirrups (B2), the highest of the typical (B1), and the lowest of the typical (B3).

For the case that contains Stirrups denser than typical (G1B1) we notice from the diagram that the resistance starts from zero and increases along with the deflection and heads towards a peak and then begins to gradually decrease as the deflection increases until a state of failure is reached.

As for the case that typically contains stirrups (G1B2), which is the second case, we notice from the diagram that the resistance increases along with the deflection until the highest value is reached. Then the resistance begins to stabilize as the deflection increases until a state of failure is reached, where a sudden drop in resistance occurs.

As for the third case (G1B3) which is the case in which they are less than the typical case, meaning the distances between them are greater, the resistance and the deviation begin to increase, but not in an almost linear manner as before, until the first peak is reached. Then the deviations begin to increase greater than the resistance increases until reaching. To the second peak point, then there is a sudden drop in resistance, then it gradually increases until a state of total failure is reached.

By matching the three curves as in Figure (11) in order to observe the role of the stirrups, we noticed that the stirrups in the typical case (G1B2) led to an elongation in the crack propagation period while maintaining an almost constant resistance, but when the stirrups were less than typical (G1B3) it gave the material Greater rigidity and resistance was directly linked to displacement with tension until the state of fracture was reached, and the material was deformed more but with insufficient resistance, in the case of stirrups higher than typical (G1B1) stirrups led to increased time and maintained resistance for the longest possible period above a certain value.

So, the role of the stirrups was clear in controlling the behavior of the beam by making the material and reinforcement work together and achieving the highest resistance for the longest possible period. it is evident that

cracking decreases with a reduction in stirrups spacing.

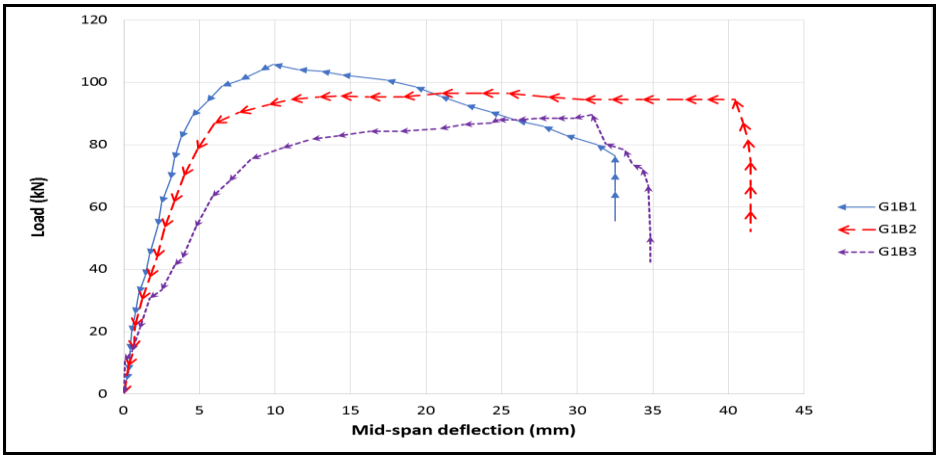

Fig 11. comparative load-displacement graph (Midpoint) for group G1.

Through the figure that shows the relationship between the width of the cracks and the load, where for the first case, in which the secondary reinforcement is larger, the cracks occurring are less, as the crack width reached 1 mm as the maximum case, and the dominant cracks were shear and bending cracks, meaning that the dominant failure mode is a combination of Shear and bending, while for the case of the typical secondary reinforcement it is also 1 mm, but with a difference in the flow of the plan, the type of cracks, and the failure state that occurred is also a combination of shear and bending. As for the third case, in which the shear reinforcement is less than ideal, we notice that the width of the cracks had reached to 3 mm, but with complete control of shear cracks, and the failure model is failure by the effect of formed shear.

Based on the results, an overarching conclusion can be derived, indicating that under standard conditions, the reinforcing stirrups render the beam susceptible to normal deformation in tension, expediting the final fracture. An increase in the number of stirrups results in enhanced resistance, yet post-fracture, due to stress concentration, the fracture undergoes acceleration. In the case of a reduced number of stirrups, the anticipated reduction in resistance is coupled with a sudden fracture occurrence. Therefore, the utilization of standard openings generally manifests a more favourable impact in this context..

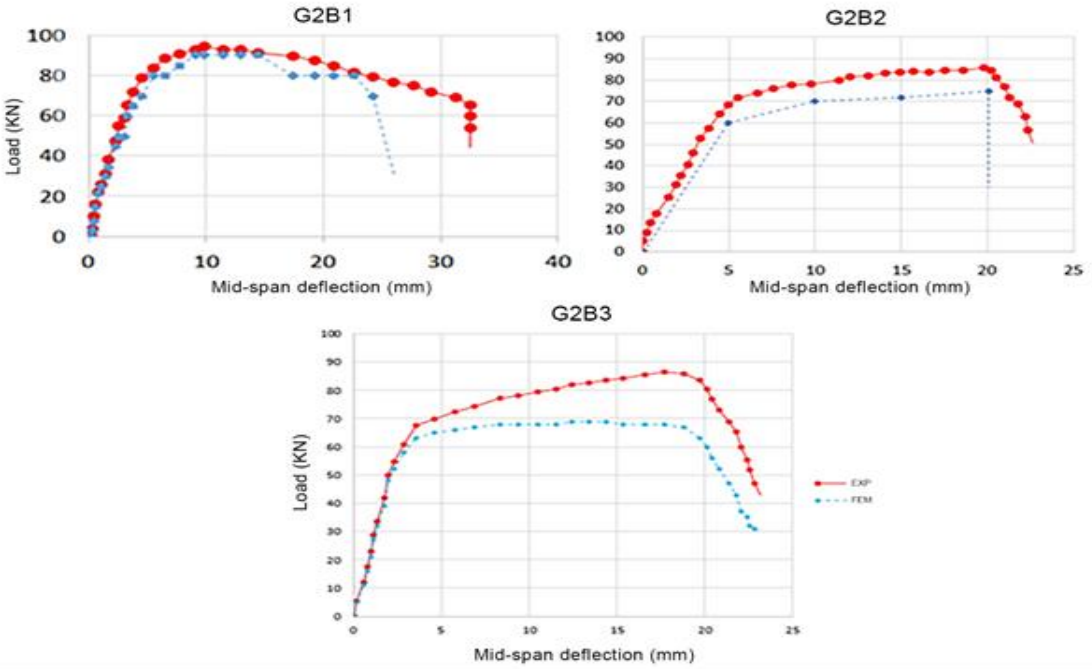

Fig 13. load-displacement graph (Midpoint) for the second group G2.

Figure (13) shows the case of the beams that were subjected to heating (G2) for which the three cases were also studied. We notice from the figure and in comparison, with the first group that was studied (G1) we find that for the case (G1B1) which calls for reinforcement of the stirrups higher than the typical one, the resistance was less. Among those in the first group, where heating led to a reduction in the value of the peak resistance that was reached while maintaining the general shape of the curve,

As for the second case, which is the typical case, (G2B2) the peak resistance also decreased, but there was no stability in the resistance and an increase in distortions. Rather, there was an increase in distortions at a greater rate than the increase in resistance, in contrast to the first group, in which the distortions increased as the resistance remained constant. For the third case, (G2B3) which is the case that is less than typical, we find that it maintained the general form of behavior but reached less resistance.

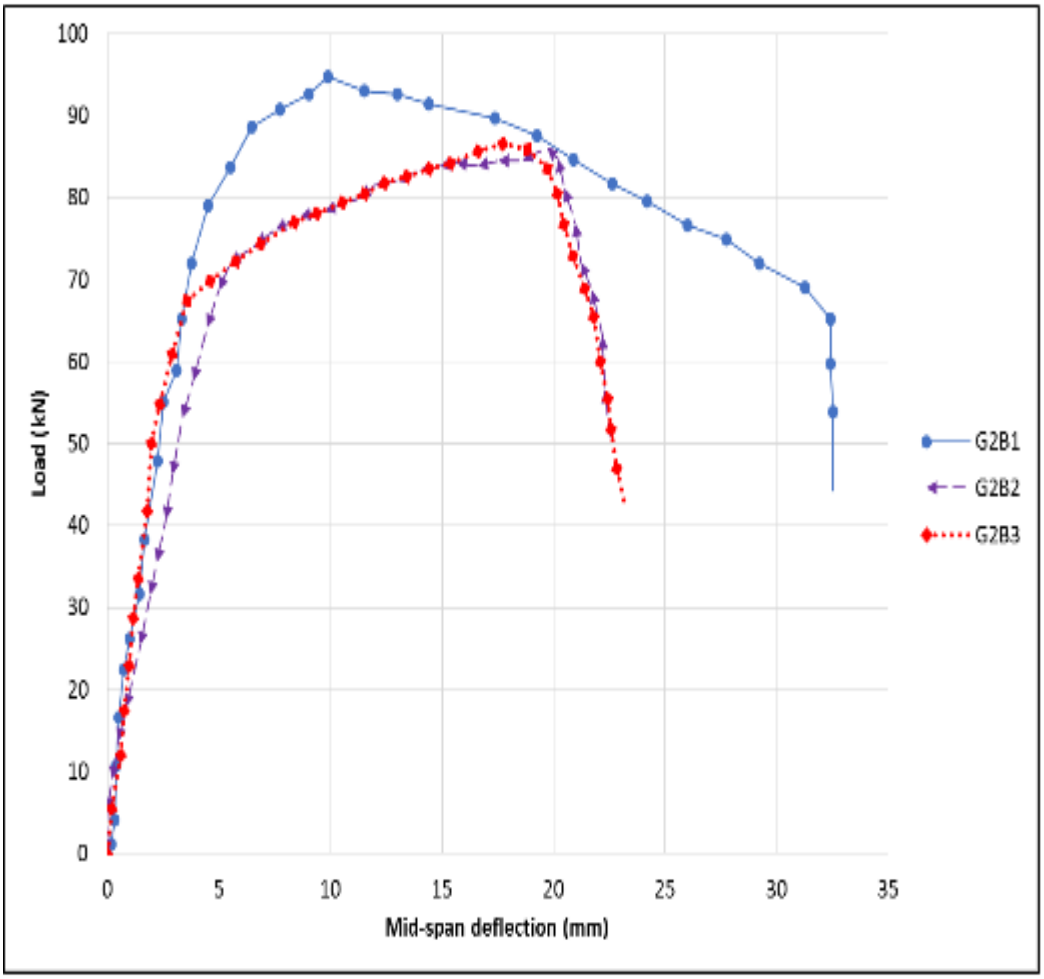

Fig 14. graphical representation comparing load-displacement (Midpoint) for group G2.

In the second group under the influence of heat, a comparison was conducted in accordance with Figure 14. It was observed that the results obtained exhibit a similarity to the previous scenario, wherein the required fracture strength increases when the number of stirrups exceeds the standard, and decreases when the number of stirrups is below the standard. In practice, severe heat diminishes the material's resistance. Exposing the beam to heat led to a decrease in the deformations exhibited by the materials and a decrease in its resistance However, in cases with a lower number of stirrups, the negative impact may not be as pronounced. Nevertheless, increasing the number of stirrups proves to be an effective strategy for enhancing the load resistance imposed on the model. Therefore, it is advisable to augment the number of stirrups to mitigate the consequences of temperature elevation, enhance deformability, and prevent abrupt fractures.

Through the figure 15 that shows the relationship between the width of the cracks and the load, where for the first case, in which the secondary reinforcement is larger, the cracks occurring are less, as the crack width reached 1 mm as the maximum case, and the dominant cracks were shear and bending cracks, meaning that the dominant failure mode is a combination of Shear and bending, while for the case of the typical secondary reinforcement it is 2 mm, more than the crack in G1 model for same model , the type of cracks, and the failure state that occurred is also a combination of shear and bending. As for the third case, in which the shear reinforcement is less than ideal, we notice that the width of the cracks had reached to 4 mm, but with complete control of shear cracks, and the failure model is failure by the effect of formed shear.

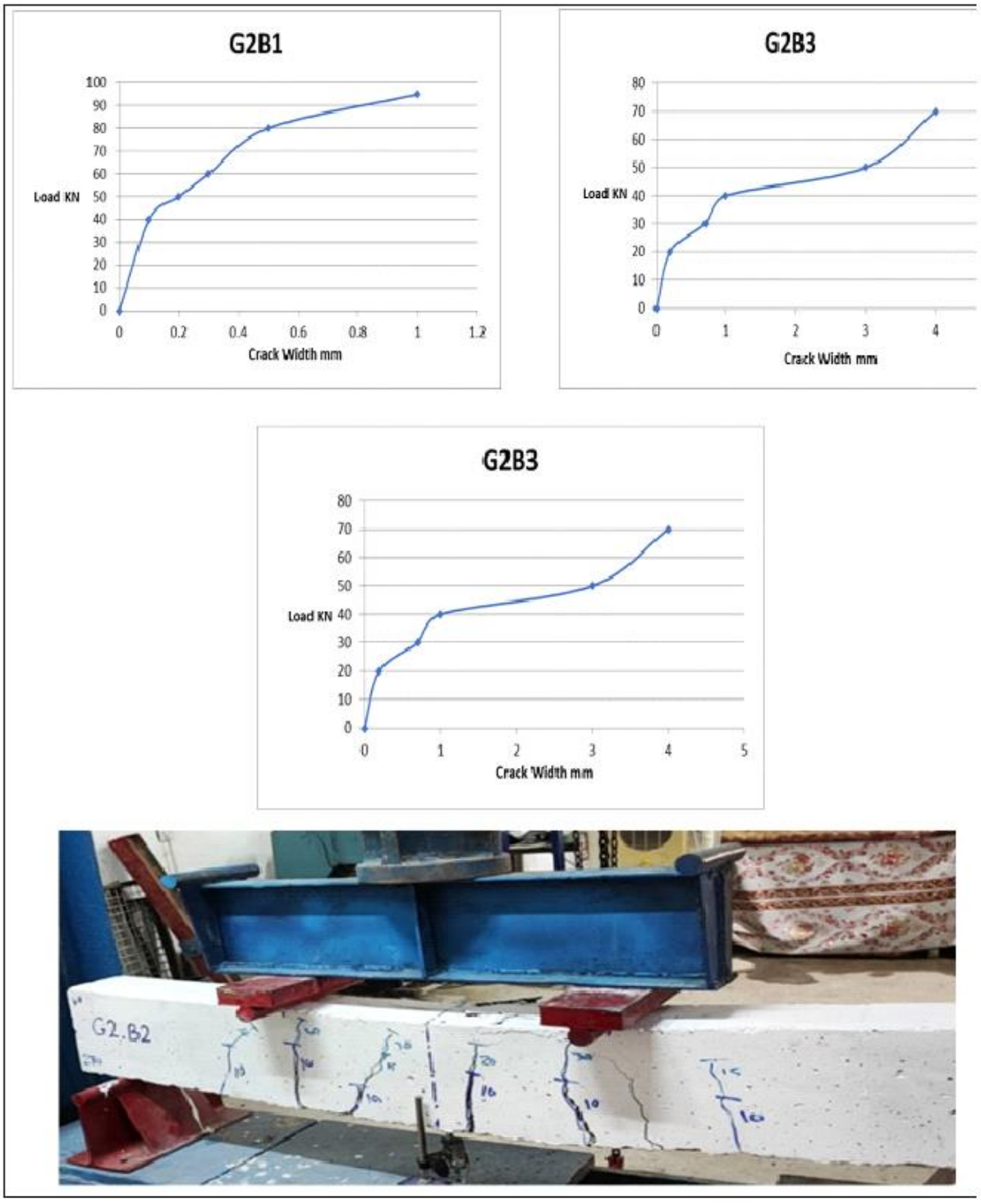

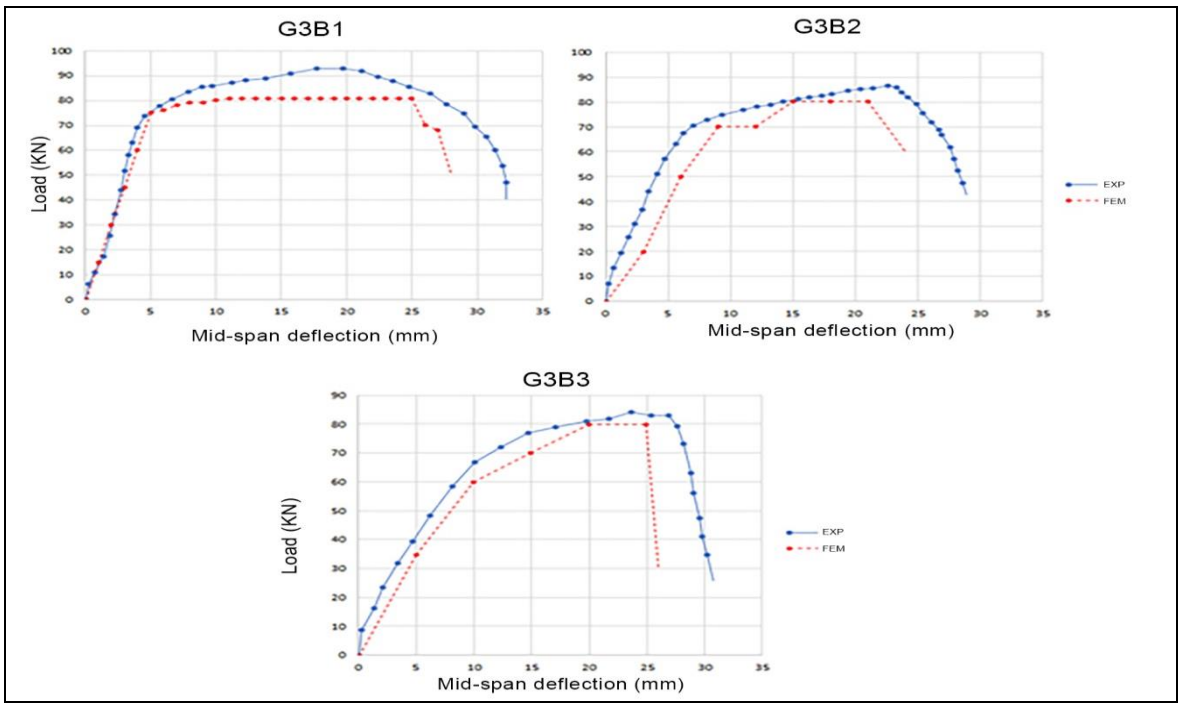

Fig 16. load-displacement graph (Midpoint) for the second group G3.

Figure 16 shows the third group (G3) in which the effect of the interaction of alkali and silica was studied. We notice a decrease in the fracture strength compared to the second group, but there was more fluidity in the curve formed and there was a greater tendency to show deformations than in the second case, where the extension of the curve was longer. The slope of the curve near failure was less severe than in the second case.
In the case where ASR was induced, the material adopted a gel-like structure with significant deformation, and it easily fractured. Additionally, the failure strength was reduced Top of Form

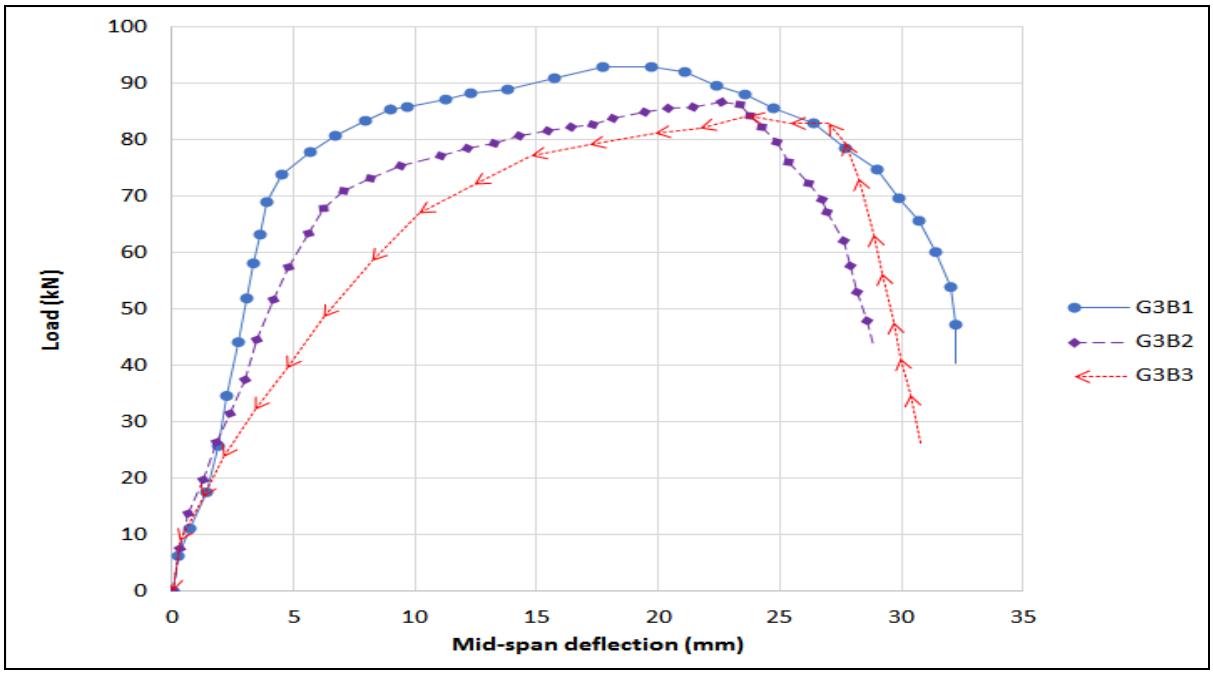

Fig 17. comparative load-displacement graph (Midpoint) for group G3.

Figure 17 illustrates the comparison between models in the third group. According to the previous explanations, an increase in the number of stirrups enhances the model's resistance. The graphs also show a more organized structure compared to previous sets, with a relative decrease in the required breaking force and an increase in the models' brittleness. The results indicate that an increase in the number of stirrups reduces the impact of ASR on the models.

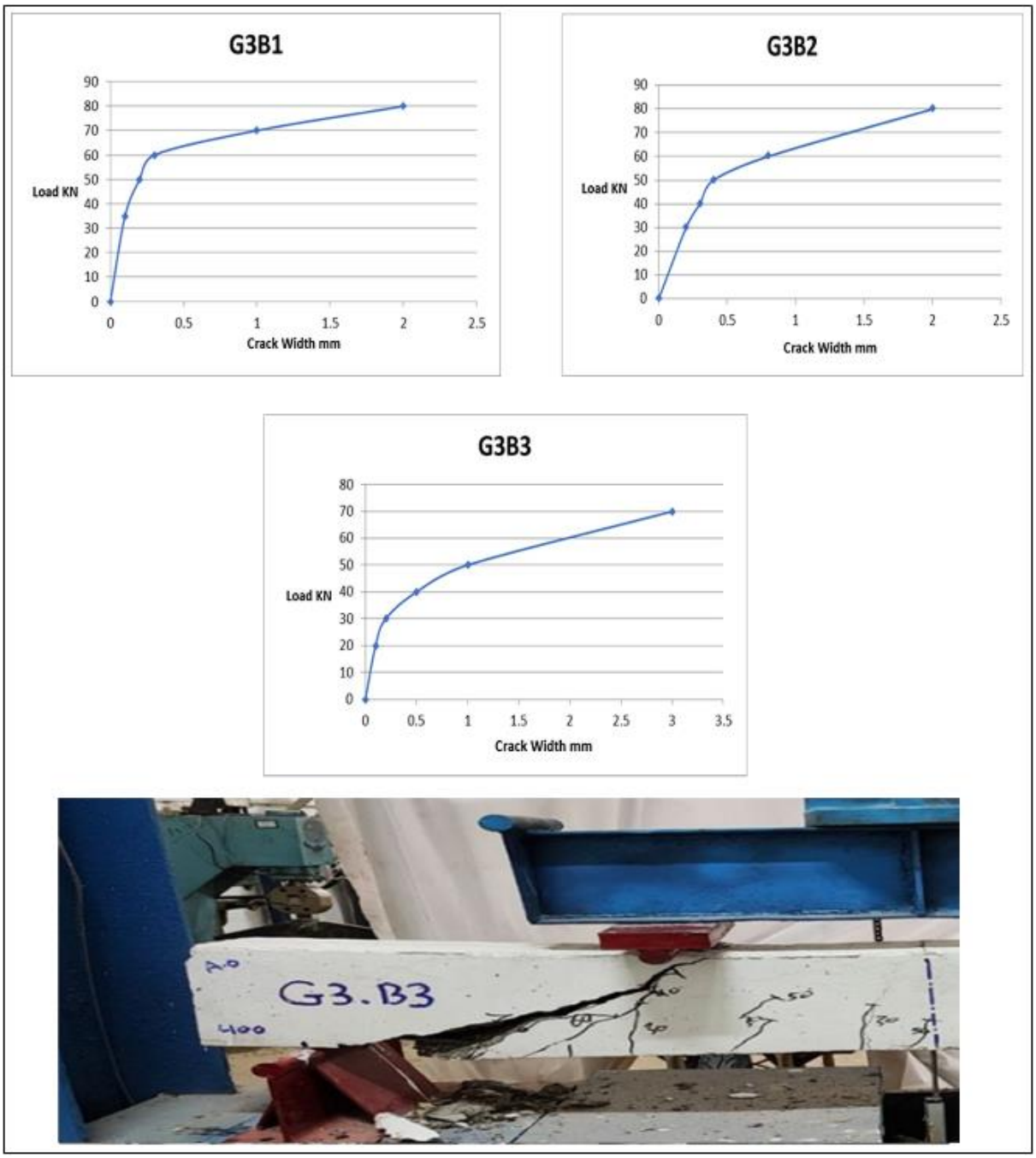

Fig 18. Crack Width For model G3

Through the figure 18 that shows the relationship between the width of the cracks and the load, where for the first case, in which the secondary reinforcement is larger, the cracks occurring are less, as the crack width reached 2mm as the maximum case, and the dominant cracks were shear and bending cracks, meaning that the dominant failure mode is a combination of Shear and bending, while for the case of the typical secondary reinforcement it is 2 mm, the type of cracks, and the failure state that occurred is also a combination of shear and

bending. As for the third case, in which the shear reinforcement is less than ideal, we notice that the width of the cracks had reached to 3 mm, but with complete control of shear cracks, and the failure model is failure by the effect of formed shear.

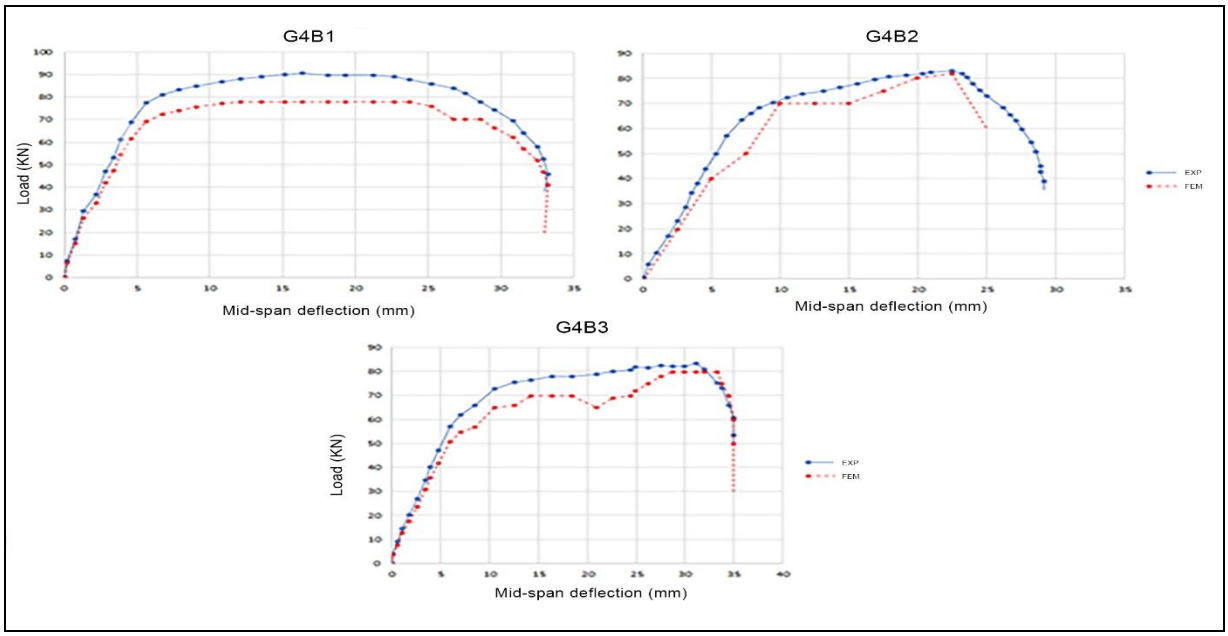

Fig 19. load-displacement graph (Midpoint) for the second group G4.

Figure 19 shows the case of the models in which silica and alkali reacted and which were subjected to heating. We note with suspicion that for the three models there was a greater decrease in resistance than the previous three groups. We note for the three cases that the three cases maintained the general shape of the curve, but with the absence of a clear peak. Where we notice the convexity of the peak.

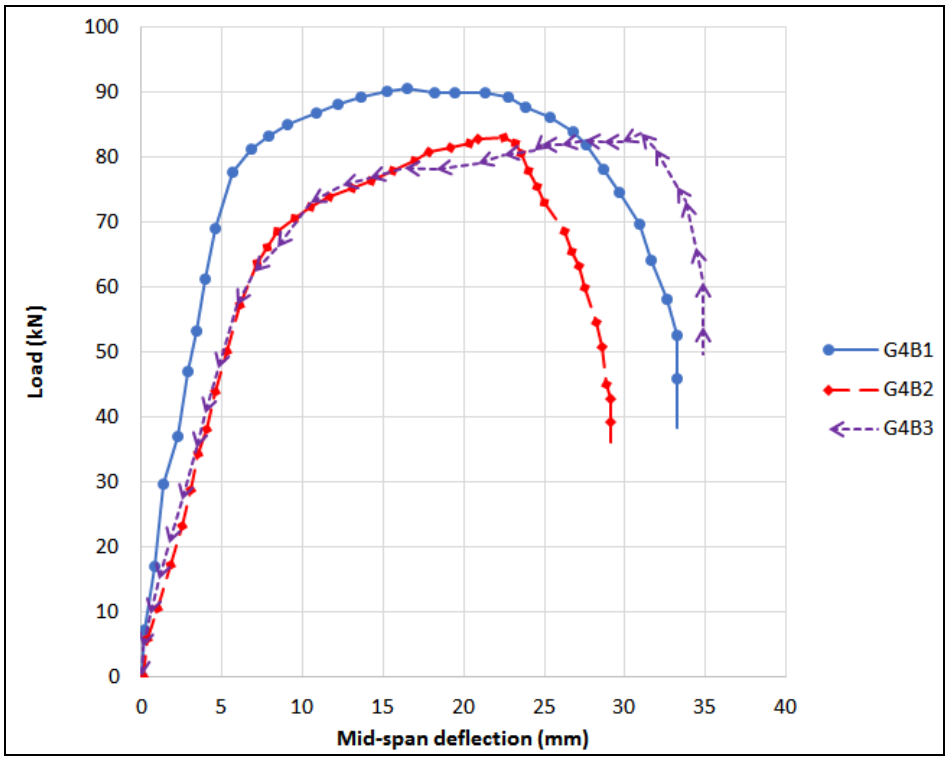

Fig 20. comparative load-displacement graph (Midpoint) for group G4.

Figure 20 illustrates that the flexural strength is higher when the number of stirrups is increased. However, reducing the number of stirrups is found to be more favourable for the standard condition. In fact, the ultimate flexural failure occurs more gradually when reducing stirrups. The optimal resistance condition is associated with an increased number of stirrups. In the standard case, stiffness increases, but flexural strength decreases. In the case of reducing stirrups, deformation is improved, as the shape becomes less resistant in the absence of self-resistance. In some way, there is better drainage. However, it is recommended to use a larger number of stirrups.

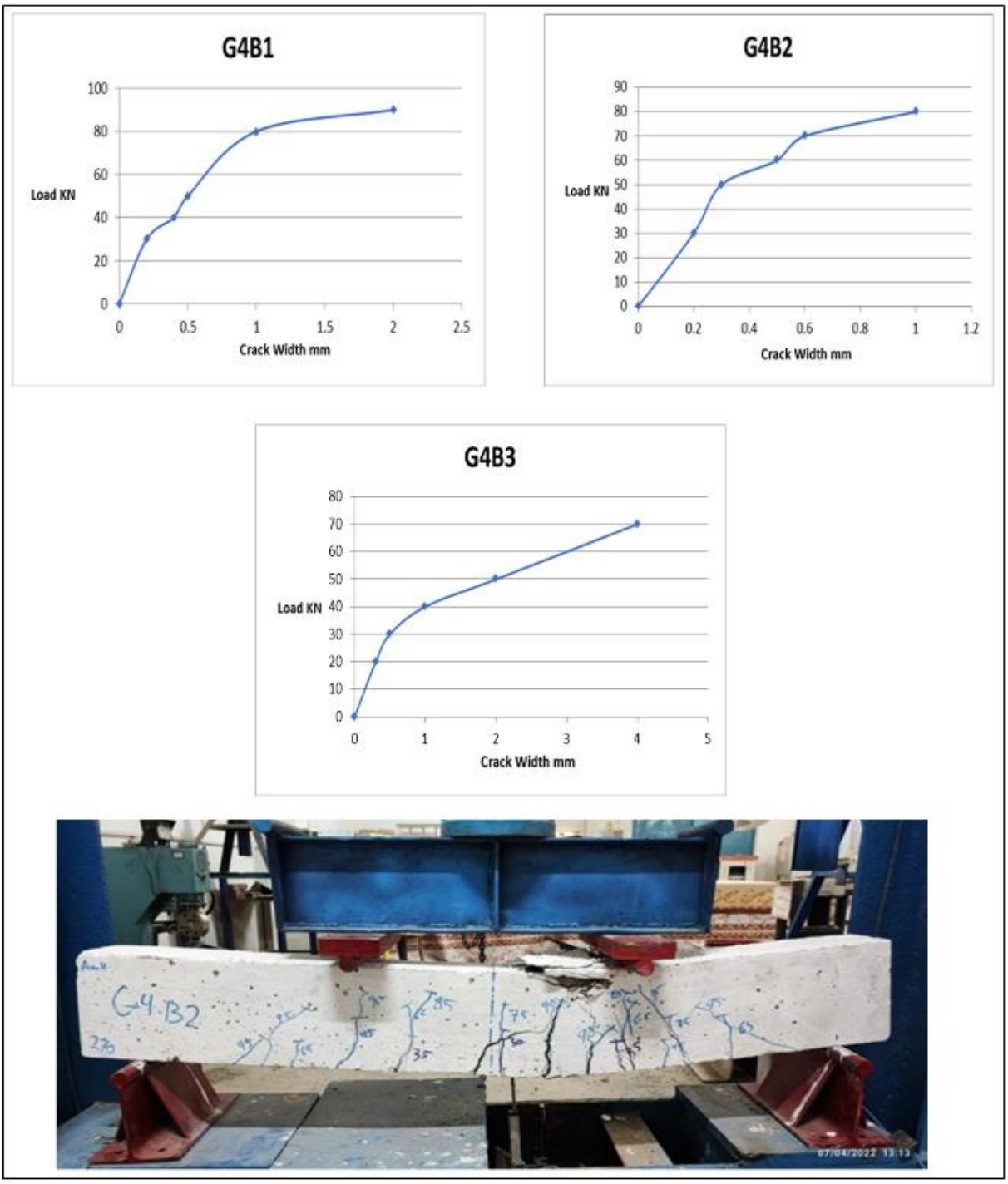

Fig 21. Crack Width for Model G4.

Through the figure 21 that shows the relationship between the width of the cracks and the load, where for the first case, in which the secondary reinforcement is larger, the cracks occurring are less, as the crack width reached 2mm as the maximum case, and the dominant cracks were shear and bending cracks, meaning that the

dominant failure mode is a combination of Shear and bending, while for the case of the typical secondary reinforcement it is 1 mm, the type of cracks, and the failure state that occurred is also a combination of shear and bending. As for the third case, in which the shear reinforcement is less than ideal, we notice that the width of the cracks had reached to 4 mm, but with complete control of shear cracks, and the failure model is failure by the effect of formed shear.

4. Conclusions:

The Figure 22 represents a comparison of all previous results for each of the experimentally examined groups and models, enabling us to deduce the following:

- Increase in temperature and the effect of Alkali-Silica Reaction (ASR) lead to a reduction in the tensile strength of the beam. ASR contributes to an increase in material deformation properties.
- Increasing the number of stirrups beyond the standard limit results in a significant increase in effective resistance.
- Reducing the number of stirrups by a certain percentage from the standard limit doesn't always lead to a reduction in material resistance.
- Standard condition of the beam unaffected by temperature or ASR experiences greater failure with displacement (midpoint).
- In cases such as earthquakes where beam deformability is crucial, reinforcement against the effects of temperature and ASR, incorporating a standard number of stirrups is recommended.
- Heating inevitably reduces the beam's resistance.
- Increasing the number of stirrups increases the force required for rupture, but beyond the rupture point, fracture accelerates.
- Nevertheless, using a larger number of stirrups is recommended.
- The combined effect of ASR and heating is more severe, although it may slightly reduce stiffness.
- Increasing the number of stirrups beyond the standard limit results in an increase in resistance.

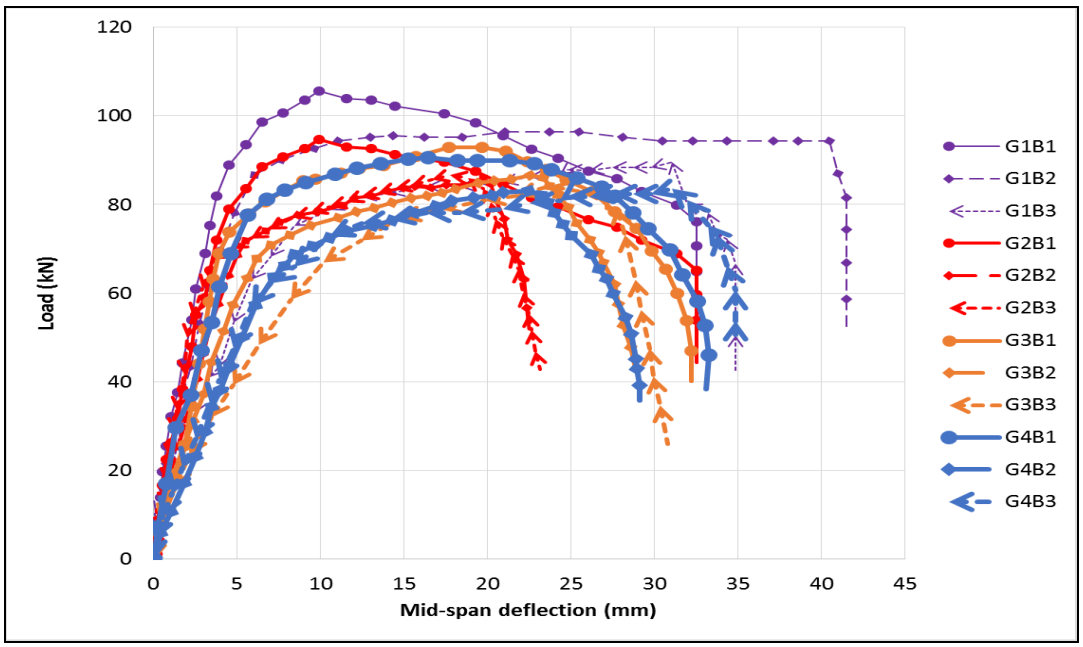

Fig 22. comparative load-displacement graph (Midpoint) for all groups.

Reference

[1] Diamond, S., & Thomas, M. (2018). Alkali–silica reaction: Mechanisms, mitigation measures, and long-term performance. Construction and Building Materials, 160, 581-593.

[2] Mehta, P. K., & Monteiro, P. J. (2017). Concrete: Microstructure, properties, and materials. McGraw-Hill Education

[3] Bentz, D. P. (2018). Effect of temperature on the microstructure of cement paste. Cement and Concrete Research, 112, 62-72.

[4] Bentz, D. P., & Stanton, T. E. (2018). Thermal stresses in concrete at early ages. Cement and Concrete Composites, 93, 149-155.

[5] Kongshaug SS, Oseland O, Kanstad T, Hendriks MAN, Rodum E, Markeset G. Experimental investigation of ASR-affected concrete – The influence of uniaxial loading on the evolution of mechanical properties, expansion and damage indices. Construction and Building Materials 648 2020.

[6] Daniela Vo et al" Evaluation of structures affected by Alkali-Silica Reaction (ASR) 2 using homogenized modelling of reinforced concrete" Elsevier. This manuscript is made available under the Elsevier user license.

[7] Fathifazl, G., & Baweja, D. (2018). Influence of elevated temperatures on mechanical properties of geopolymer paste, mortar, and concrete. Cement and Concrete Research, 114, 21-31.

[8] Pantazopoulou, S. J., & Vassiliou, M. F. (2017). The effect of temperature on high-performance concrete: A literature review. ACI Materials Journal, 114(3), 513-522.

[9] Al-Swaidani, A. M., Almusallam, T. H., & Maslehuddin, M. (2018). Effect of elevated temperature on the mechanical properties and behavior of plain and fibre reinforced high-strength concrete. Construction and Building Materials, 170, 184-199

[10] Ismail, M., & Wafa, F. (2019). Review of mechanical properties of high-strength concrete after exposure to elevated temperatures. Journal of Materials in Civil Engineering, 31(2), 04018386.

[11] Bentz, D. P., & Ferraris, C. F. (2018). The effects of temperature on the transport properties of concrete. Cement and Concrete Research, 111, 78-87.

[12] Pan, Z., Wu, H., Gao, S., & Shi, X. (2019). Effects of high temperatures on mechanical properties of concrete containing supplementary cementitious materials: A review. Construction and Building Materials, 184, 160-177.

[13] Bentur, A., & Mindess, S. (2019). Fibre reinforced cementitious composites (2nd ed.). Taylor & Francis.

[14] ACI Committee 318, "Building Code Requirements for Structural Concrete (ACI 318-19) and Commentary," American Concrete Institute, 2019.

[15] American Society for Testing and Materials (2007) ASTM C 1260-07; Standard Test Method for Potential Reactivity of Aggregates (Mortar-Bar Method)1, ASTM, Philadelphia, 1-5.

[16] Dixon, Donald E., Jack R. Prestrera, George RU Burg, Subcommittee A. Chairman, Edward A. Abdun-Nur, Stanley G. Barton, Leonard W. Bell et al. Standard Practice for Selecting Proportions for Normal, Heavyweight, and Mass Concrete, (ACI 211.1-91). (1991) Reapproved (2002).

[17] ASTM C150/C150-07. Standard Specification for Portland Cement, American Society for Testing and Materials. 4 (2) (2007).

[18] ASTM C33/C33M-16. Standard specification for concrete aggregate, American Society for Testing and Materials. (2016).

[19] ASTM C 494/C494-05. Standard specification for chemical admixtures for concrete, American Society for Testing and Materials. (2005).

[20] ASTM C143 /143-05. Standard Test Method for Slump of Hydraulic Cement Concrete, American Society for Testing and Materials. (2005).

[21] John F. Bonacci, Sergio M. Alcocer. Recommendations for Design of Beam-Column Connections in Monolithic Reinforced Concrete Structures, American Concrete Institute. ACI 352R-02 (2002) P.37.

[22] ASTM A615/AM615-15. Standard Specification for Deformed and Plain Carbon-Steel Bars for Concrete Reinforcement, American Society for Testing and Materials. (2015)

[23] ACI Committee 318. (2014). ACI 318-14: Building Code Requirements for Structural Concrete. American Concrete Institute.

[24] Nilson, A. H., Darwin, D., & Dolan, C. W. (2019). Design of Concrete Structures. McGraw-Hill Education.
[25] Subramanian, N. (2016). Concrete Structures: Stresses and Deformations: Analysis and Design for Serviceability. CRC Press.
[26] Wight, J. K., & MacGregor, J. G. (2012). Reinforced Concrete Mechanics and Design. Pearson.
[27] Mindess, S., Young, J. F., & Darwin, D. (2015). Concrete. Pearson.
[28] Mehta, P. K., & Monteiro, P. J. M. (2019). Concrete: Microstructure, Properties, and Materials. McGraw-Hill Education.
[29] Nawy, E. G. (2019). Concrete Construction Engineering Handbook. CRC Press.
[30] Neville, A. M. (2016). Properties of Concrete. John Wiley & Sons.